수의학 석사 학위논문

UCP2 Deletion Downregulates Adipocyte Apoptosis and Prevents Diet-Induced Obesity

2022년 08월

서울대학교 대학원

수의학과 수의생명과학 전공

김 도 현

A Dissertation for the Degree of Master of Science

UCP2 Deletion Downregulates Adipocyte Apoptosis and Prevents Diet-Induced Obesity

August 2022

Do Hyun Kim

Supervisor: Prof. Je Kyung Seong, D.V.M., Ph.D.

Department of Veterinary Medicine

College of Veterinary Medicine

Developmental Biology and Genomics

The Graduate School of Seoul National University

UCP2 Deletion Downregulates Adipocyte Apoptosis and Prevents Diet-Induced Obesity

지도교수 성 제 경

이 논문을 수의학석사 학위논문으로 제출함

2022 년 5 월

서울대학교 대학원

수의학과 수의생명과학 전공

김 도 현

김도현의 수의학석사 위논문을 인준함

2022 년 7 월

위 원 장 윤 여 성 **(인)**

부위원장 성 제 경 **(인)**

위 원 오 승 현 **(인)**

Abstract

UCP2 Deletion Downregulates Adipocyte Apoptosis and Prevents Diet-Induced Obesity

Do Hyun Kim

College of Veterinary Medicine

Developmental Biology and Genomics

The Graduate School

Seoul National University

Uncoupling protein 2 (UCP2) was first introduced as a member of Uncoupling protein family and a regulator of ROS formation; however, its role in adipose tissue is not fully understood. In the present study, I have investigated the role of UCP2 against high-fat diet (HFD)-induced obesity in epididymal white adipose tissue (eWAT) and browning of inguinal white adipose tissue (iWAT). Diet-induced obesity is closely related to macrophage infiltration and the secretion of pro-inflammatory cytokines. Macrophages surround adipocytes and form a crown-like-

structure (CLS). Some reports have suggested that CLS formation requires adipocyte apoptosis. After 12 weeks of HFD challenge, UCP2 knockout (KO) mice maintained relatively lean phenotypes compared to wild-type (WT) mice. In eWAT, UCP2 deletion reduces macrophage infiltration, CLS formation, and inflammatory cytokines after the HFD challenge. Surprisingly, I found that apoptotic signals were also reduced in the UCP2 KO mice. This study suggests that UCP2 deficiency may prevent diet-induced obesity by regulating adipocyte apoptosis. However, UCP2 deficiency did not affect the browning capacity of iWAT.

Keyword: Uncoupling Protein 2, obesity, adipose tissue inflammation, CLS, mouse, apoptosis
Student Number: 2020-23775

List of Abbreviation

ATM	Adipose tissue macrophage
BAT	Brown adipose tissue
Bax	BCL2 associated X
BCL2	B-cell lymphoma 2
Cas3	Caspase 3
Cas9	Caspase 9
Cidea	Cell death-inducing DFFA effector A
CLS	Crown-like-structure
DIO	Diet-induced-obesity
eWAT	Epididymal white adipose tissue
Elovl3	ELOVL Fatty acid elongase 3
HFD	High fat diet
H&E	Hematoxylin and eosin
IFNα	Interferon alpha
IL-1β	Interleukin 1 beta

IHC	Immunohistochemistry
iWAT	Inguinal white adipose tissue
KO	Knockout
NCD	Normal chow diet
Pgc1α	Peroxisome proliferator-activated receptor-gamma coactivator
Pparγ	Peroxisome proliferator-activated receptor gamma
ROS	Reactive oxygen species
SNS	Sympathetic nervous system
SVF	Stromal vascular fraction
TG	Triglyceride
TNFα	Tumor necrosis factor-alpha
UCP1	Uncoupling protein 1
UCP2	Uncoupling protein 2
WT	Wild type

WAT	White adipose tissue

Contents

LIST OF FIGURES

LIST OF TABLE

INTRODUCTION

Uncoupling protein 2 (UCP2) is encoded by a mitochondrial gene and was first reported as a regulator of mitochondrial proton leakage, ATP production, and insulin secretion (Zhang et al., 2001). Although the exact mechanisms underlying these functions have not yet been understood, many researchers have agreed that *UCP2* expression is negatively correlated with ROS and NO production (Arsenijevic et al., 2000; Bai et al., 2005). In addition, the lifespan of Uncoupling protein 2 (UCP2) knock-out (KO) mice is shorter than that of wild-type (WT) mice (Andrews & Horvath, 2009). However, UCP2 displays a wide tissue expression range (Erlanson-Albertsson, 2002) and its roles in various tissues and cell types have not been covered.

Adipose tissue is a major metabolic organ that stores energy in the form of triglycerides (Choe et al., 2016; Cohen & Spiegelman, 2016). Its function in energy homeostasis of the whole body has been studied for decades and it is now considered an endocrine organ that secretes various adipokines and lipid metabolites (Lee et al., 2013; Prunet-Marcassus et al., 2006). Another key aspect of adipose tissue is the thermogenic capacity (Bartelt & Heeren, 2014; Himms-Hagen, 1985) of brown adipose tissue (BAT), which means dissipation of excess energy in the form of heat. The activation of BAT and recruitment of beige adipocytes from white adipocytes occur in an uncoupling protein 1 (UCP1)-dependent manner (Fedorenko et al., 2012; Madsen et al., 2010).

Recently, a study has revealed that macrophage-specific deletion of UCP2 does not affect adipose tissue inflammation or weight gain after a high-fat diet (HFD) (van Dierendonck et al., 2020). To study the role of UCP2 in adipose tissue, I have examined HFD-induced obesity and β3 adrenergic stimulation in UCP2 KO mice. I have demonstrated that UCP2 deletion dysregulates adipose tissue homeostasis under diet-induced obesity (DIO), but does not affect the browning of white adipose tissue (WAT).

This study also showed that UCP2 deletion alleviates HFD-induced weight gain and adipose tissue inflammation by blocking adipocyte apoptosis, an event preceding the recruitment of macrophages and proinflammatory cytokine secretion. I also establish the role of UCP2 in thermogenesis and browning of inguinal white adipose tissue (iWAT), a well-known function of UCP1, from the same family. Under β3-specific stimulation or 4 °C cold exposure, browning capacity of iWAT of UCP2 deficient mice was comparable to that of WT mice.

MATERIALS AND METHODS

Animal Experiment

UCP2 null KO mice were purchased from the Jackson Laboratory, USA. (B6.129S4-UCP2tm1Lowl/J, Strain #:005934). UCP2 KO mice were obtained by crossing heterozygous breeders. All protocols were performed in accordance with the Guide for Animal Experiments (approved by the Institutional Animal Care and Use Committee of Seoul National University, Seoul, Korea) (approval number: SNU-201013-2-1). For HFD experiments, 6-week-old male WT and KO mice were randomly assigned (n = 5) to either NCD or a 60% HFD (20% carbohydrate, 60% fat, 20% protein; D12492; Research Diets Inc.). For CL 316,243 (Sigma, USA) treatment, 7-week-old WT and KO mice were i.p. injected with 1 mg/kg of CL for 3 days (n = 4). For the cold challenge, 7-week-old WT and KO mice were randomly assigned to either thermoneutral (30 °C) or cold (4 °C) environment conditions for 5 consecutive days (n = 5). At the end of each experiment, the body composition of all animals was determined by nuclear magnetic resonance (Minispec LF-50, Bruke).

H&E and Immunohistochemistry (IHC) Staining

Samples were fixed with 4% paraformaldehyde (HP2031, Biosesang, Korea) and embedded in paraffin. They were sliced into 4.5-μm-thin sections and stained with H&E, following a standard protocol. For IHC staining, anti-F4/80 antibody (D2S9R, Cell Signaling Technology, Massachusetts, USA) and anti-

UCP1 antibody (Abcam, Cambridge, UK) were used. The samples were then washed and blocked with 2.5% horse serum for 1 h. After another washing with PBS + 0.05% Tween 20 incubation was performed with a 1:500 dilution of primary anti-F4/80 overnight in a 4 °C chamber. Samples were washed and incubated with secondary antibody (ImmPRESS, Vector Laboratories, California, USA) for 1 h at 24 °C. Finally, they were developed using a DAB kit (Vector Laboratories, California, USA). H&E and IHC samples were visualized using a Pannoramic Scanner (3DHISTECH, Budapest, Hungary).

Protein analysis

Proteins were extracted using RIPA buffer and quantified using the BCA assay protocol. Equal amounts of protein were separated by SDS-PAGE and then transferred to PVDF membranes. Samples were incubated with primary antibodies overnight at 4 °C and then incubated with HRP-conjugated secondary antibodies. The blots were visualized using enhanced chemiluminescence and a Chemi-Doc Imaging System (Bio-Rad, California, USA). Images were quantified and normalized using the ImageJ software (NIH, New York, USA). The primary antibodies used were UCP1 (Abcam, Cambridge, UK), Caspase3 (Cell Signaling Technology, Massachusetts, USA), Cleaved caspase 3 (Cell Signaling Technology, Massachusetts, USA), α-actin (Sigma, Misouri, USA), and β-tubulin (Abbkine, Wuhan, China).

RNA extract and Quantitative real-time PCR

Total RNA was extracted from the tissues using TRIzol reagent (Invitrogen, Massachusetts, USA) according to the manufacturer's instructions. cDNA was synthesized using a premix (Bioneer, Daejeon, Korea). qPCR was performed using the QuantStudio5 (Applied Biosystems, Massachusetts, USA). PCR was performed using the SYBR Lo-ROX Kit (Meridian Bioscience, Ohio, USA), according to the manufacturer's instructions. The primer sequences used are shown in Table 1.

Table 1. Primers used for qRT-PCR analysis

Primer	Forward primers	Reverse primers
Ucp2	TTAAGTGTTTCGTCTCCCAGCC	ACTCTGCCGGAGTTCTGGA
Pparγ	TGAAAGAAGCGGTGAACCACTG	TGGCATCTCTGTGTCAACCATG
TNFα	CCCTCACACTCAGATCATCTTCT	GCTACGACGTGGGCTACAG
IFNγ	TCAAGTGGCATAGATGTGGAAGAA	TGGCTCTGCAGGATTTTCATG
IL-1β	GCAACTGTTCCTGAACTCAACT	ATCTTTTGGGGTCCGTCAACT
Adiponectin	TGACGACACCAAAAGGGCTC	ACCTGCACAAGTTCCCTTGG
IL-10	GCTCTTACTGACTGGCATGAG	CGCAGCTCTAGGAGCATGTG
CCL2	TTAAAAACCTGGATCGGAACCAA	GCATTAGCTTCAGATTTACGGGT
Cas3	TGGGAGCAAGTCAGTGGA	CACCATGGCTTAGAATCA
Cas9	TTCCCAGGTTTTGTCTCCTG	GGGACTGCAGGTCTTCAGAG
Bax	TGCAGAGGATGATTGCTGAC	GATCAGCTCGGGCACTTTAG
BCL2	CTGCAAATGCTGGACTGAAA	TCAGGAGGGTTTCCAGATTG
Ucp1	ACTGCCACACCTCCAGTCATT	CTTTGGCTCACTCAGGATTGG
Elovl3	TTCTCACGCGGGTTAAAAATGG	GAGCAACAGATAGACGACCAC
Cidea	TGCTCTTCTGTATCGCCCAGT	GCCGTGTTAAGGAATCTGCTG
Pgc1α	CCCTGCCATTGTTAAGACC	TGCTGCTGTTCCTGTTTTC
36B4	GAGGAATCAGATGAGGATATGGGA	AAGCAGGCTGACTTGGTTGC

RESULTS

UCP2 mRNA expressions in KO mice and adipocytes

I first confirmed that UCP2 mRNA expression was downregulated in the lung, iWAT, and eWAT of UCP2 KO mice (Fig. 1A, 1B, 1C). To investigate the role of UCP2 in adipose tissue under HFD condition, 6-week-old C57BL/7 mice were fed eitxher normal chow diet (NCD) or high-fat diet for either 2 or 16 weeks. I then isolated adipocytes and stromal vascular fraction (SVF) from epididymal white adipose tissue (eWAT) and measured UCP2 mRNA levels (Fig. 2A, 2B). UCP2 expression was significantly increased in adipocytes when challenged with HFD. To confirm UCP2 expression in adipocytes, I used a 3T3L1 cell line and verified a positive correlation between mRNA levels of UCP2 and Pparγ, a differentiation marker (Fig. 2C, 2D).

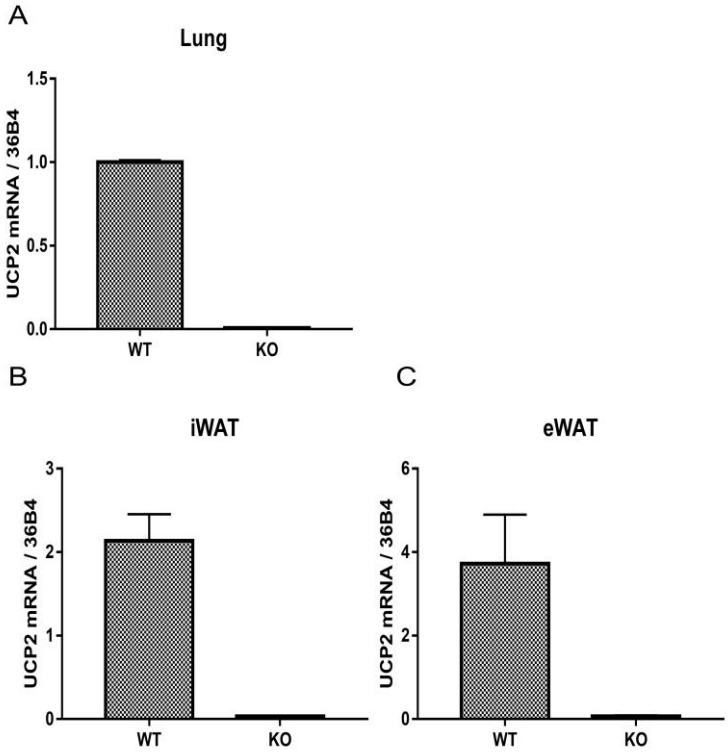

Figure 1. UCP2 KO confirmation by qPCR analysis.

(A) qRT-PCR analysis showed that UCP2 mRNA expression was down regulated in the stomach, (B) iWAT, and (C) eWAT in KO mice. Data are presented as the mean ± SEM. *$p < 0.05$, **$p < 0.01$, ***$p < 0.001$.

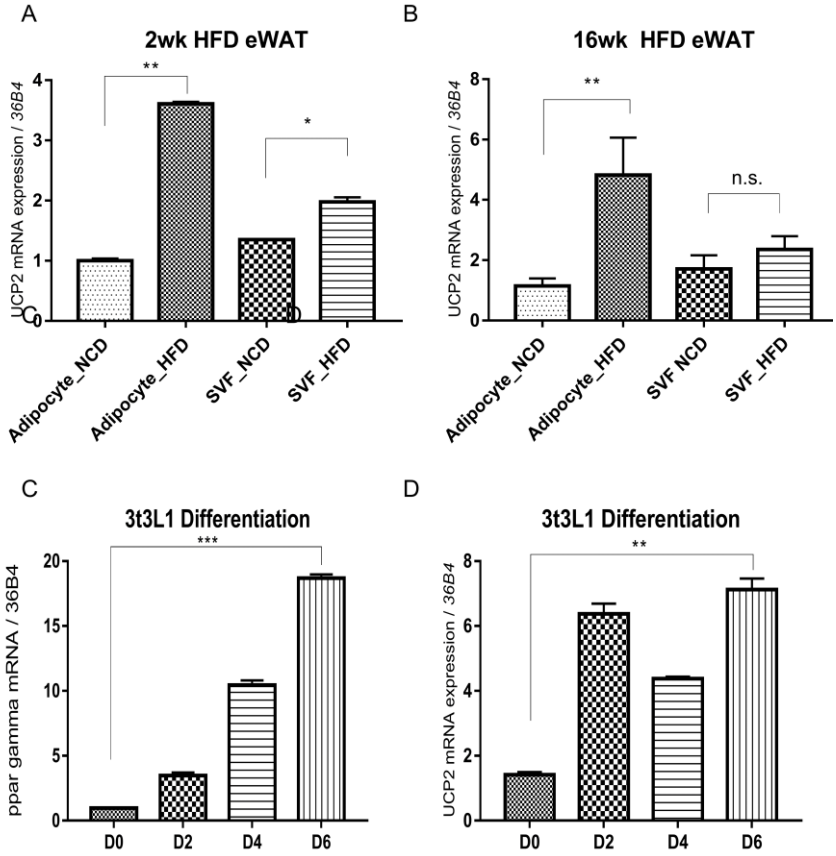

Figure 2. UCP2 mRNA expressions in adipocytes and SVF under HFD challenge.

qRT-PCR showed UCP2 mRNA expression in adipocyte and SVF from eWAT after (A) 2weeks or (B) 16 weeks of HFD challenge. (C) Pparγ, a differentiation marker, mRNA expression levels of 3T3L1. (D) UCP2 mRNA expressions as 3T3L1 differentiate.

Data are presented as the mean ± SEM. *$p < 0.05$, **$p < 0.01$, ***$p < 0.001$.

UCP2 KO mice were protected from HFD induced obesity

Then, 6-week-old WT and KO mice were fed either NCD or HFD for 12 weeks. A chronic access to HFD resulted in significant weight gain in WT mice compared to mice with NCD, whereas the weight gain in HFD KO mice was comparable to that in NCD group (Fig. 3A, 3B). The net body weight change by the NCD or HFD administration was also significantly less in the KO group (Fig. 3C). Body composition data also coincided with the changes in body weight. UCP2 KO mice showed significantly lower fat mass and higher lean mass than WT mice (Fig. 4A). WAT in KO mice was lesser than it was in WT mice (Fig. 4B). The WAT weight of HFD KO mice was significantly lower than that of HFD WT mice (Fig. 4C). Serum triglyceride (TG) and glucose levels were also lower in HFD KO mice than in HFD WT mice (Fig. 5A, 5B). The mRNA level of the eWAT glucose uptake marker, Glut4, was increased in HFD KO mice compared to that in NCD KO mice, but the expression level in HFD KO mice was also significantly lower than that in HFD WT mice (Fig. 5C). Hematoxylin and eosin (H&E) staining also revealed that adipocytes were smaller in HFD KO mice (Fig. 6A, 6B).

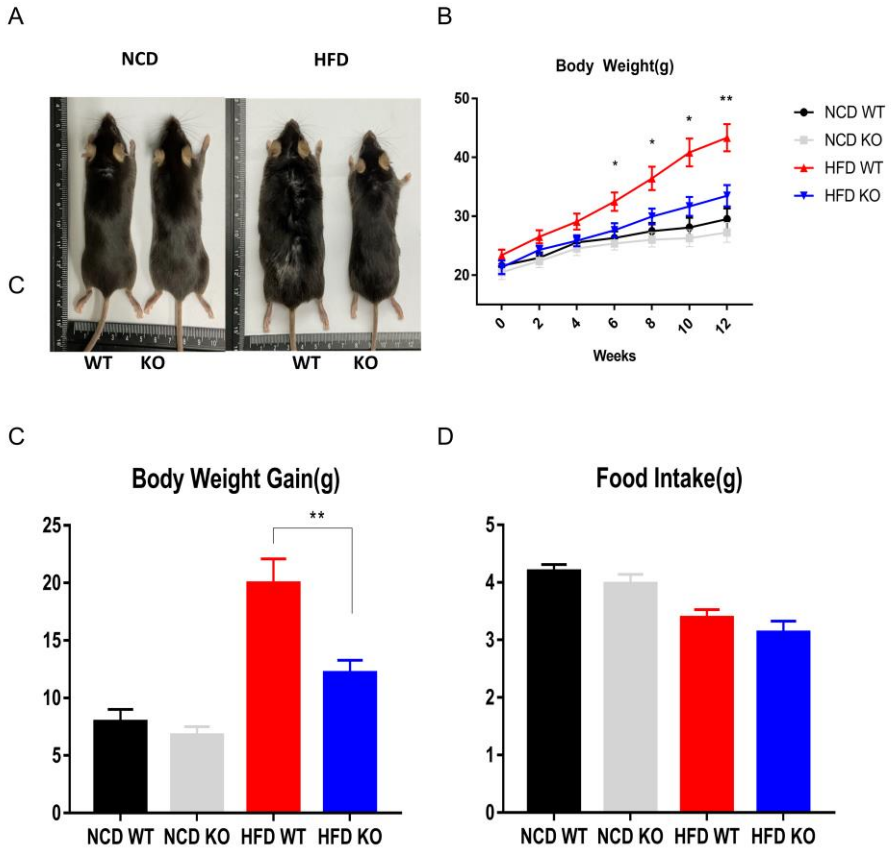

Figure 3. UCP2 deletion decreases body weights after the HFD challenge. (A) Photographs of WT and KO mice after 12 weeks of NCD and HFD. (B) Bodyweight graph from 6-week to eighteen-week-old mice of each group. (C) Food Intake was comparable in NCD and HFD groups. (D) Net body weight gain graphs were shown. Data are presented as the mean ± SEM. *$p < 0.05$, **$p < 0.01$, ***$p < 0.001$.

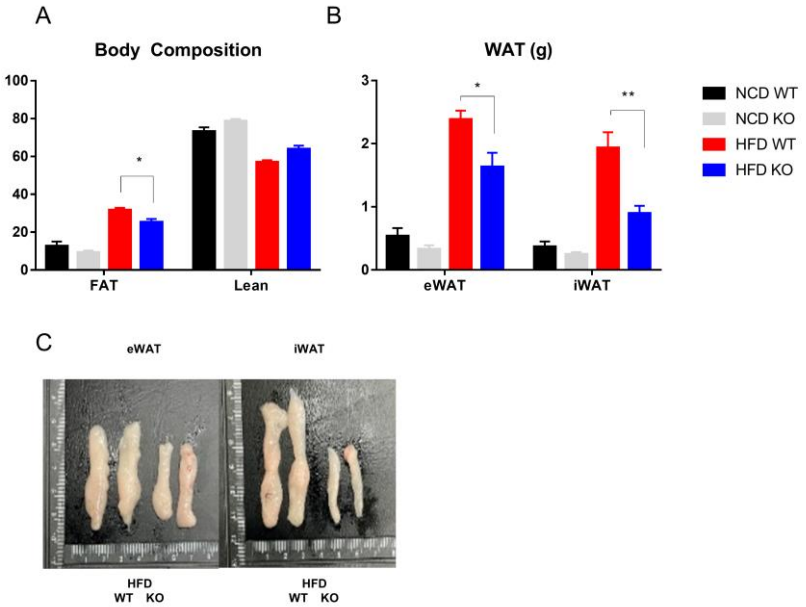

Figure 4. UCP2 deletion decreases fat mass after the HFD challenge.

(A) Body composition data after 8 weeks of HFD challenge. (B) Weights of eWAT and iWAT were graphed. (C) Photographs of eWAT and iWAT of UCP2 WT and KO mice. Data are presented as the mean ± SEM. *$p < 0.05$, **$p < 0.01$, ***$p < 0.001$.

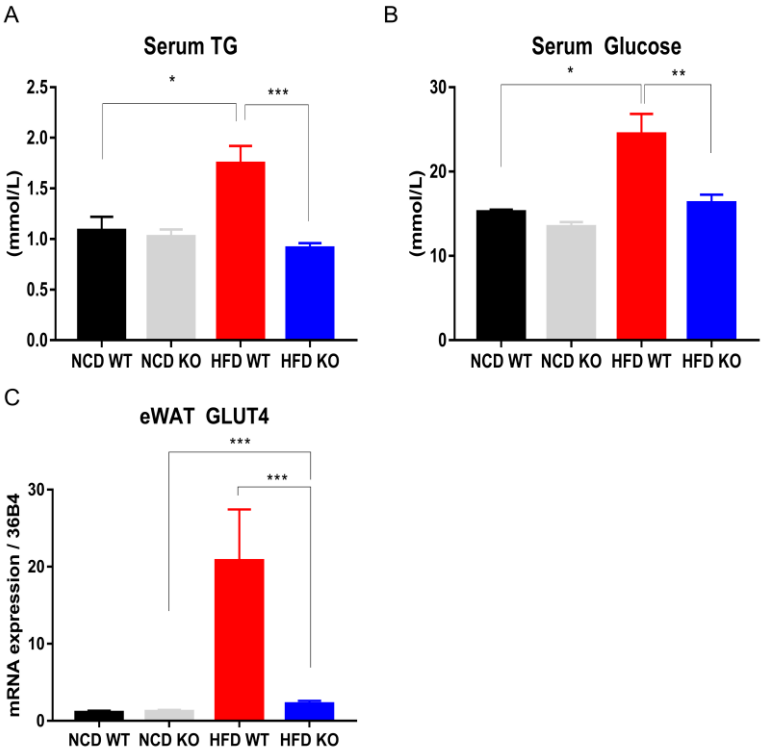

Figure 5. UCP2 deletion reduces serum TG and Glucose level.

(A) Serum Triglyceride levels after 8 weeks of HFD challenge. (B) Serum glucose levels after 8 weeks of HFD challenge. (C) qRT-PCR analysis showed GLUT4 mRNA expression. Data are presented as the mean ± SEM. *$p < 0.05$, **$p < 0.01$, ***$p < 0.001$.

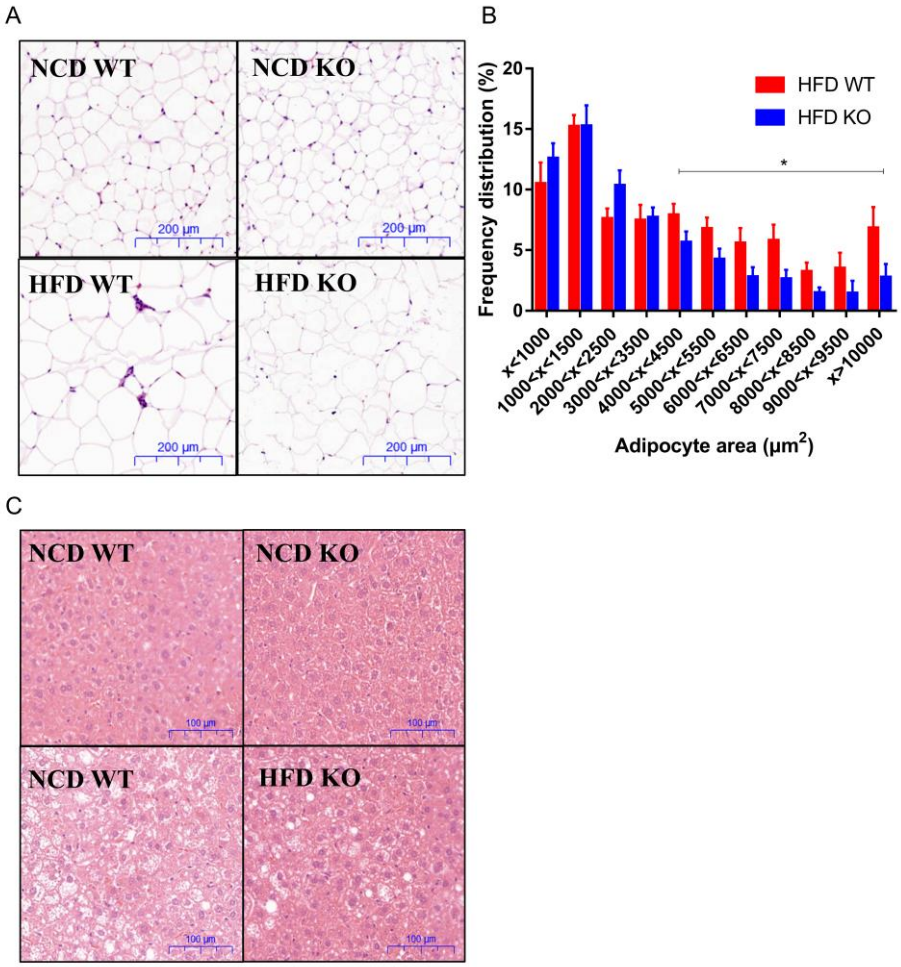

Figure 6. UCP2 deletion reduces adipocyte sizes and lipid droplets in the liver after the HFD challenge.

(A) H&E staining slides of epididymal adipose tissue. (B) Average adipocyte sizes after challenge. (C) H&E staining slides of liver. Data are presented as the mean ± SEM. *$p < 0.05$, **$p < 0.01$, ***$p < 0.001$.

HFD-induced macrophage infiltration and inflammation were reduced in HFD KO mice.

As HFD-induced obesity is closely linked to macrophage infiltration and secretion of pro-inflammatory cytokines (Trayhurn, 2007; Weisberg et al., 2003), I analyzed the macrophages present in epididymal adipose tissue. Localization of antigen F4/80 using immunohistochemistry (IHC) staining showed crown-like-structure (CLS) formation in macrophages (Fig. 7A), and the number of CLSs was comparable in NCD WT and KO mice, while HFD KO mice showed a significant reduction in CLS formation compared to HFD WT (Fig. 7B). The mRNA level of *CCL2*, a marker for macrophage recruitment to adipose tissue, was significantly reduced in HFD KO mice compared to that in HFD WT mice (Fig. 9B). Additionally, mRNA levels of pro-inflammatory markers, TNFα, IFNγ, and IL-1β were also significantly decreased in KO mice (Fig. 8A, 8B, 8C), and mRNA level of the anti-inflammatory marker adiponectin in both HFD groups was similarly reduced, compared to that in NCD groups (Fig. 9A). Many studies have shown that in DIO, adipocyte apoptosis is a major cause of and a direct upstream step before CLS formation (Alkhouri et al., 2010; Lindhorst et al., 2021; Xiao et al., 2010). To determine whether deletion of the *UCP2* gene affects CLS formation

and secretion of cytokines directly, or an upstream event, I investigated mRNA and protein levels of apoptotic signals in adipose tissue. I observed that caspase 3 (Cas3), caspase 9 (Cas9), and Bax/BCL2, the major apoptosis markers, only increased in the HFD WT group (Fig. 10A, 10B, 10C). TUNEL assay was also performed, and apoptotic expression was higher in HFD WT mice compared to that in KO mice (Fig. 13A).

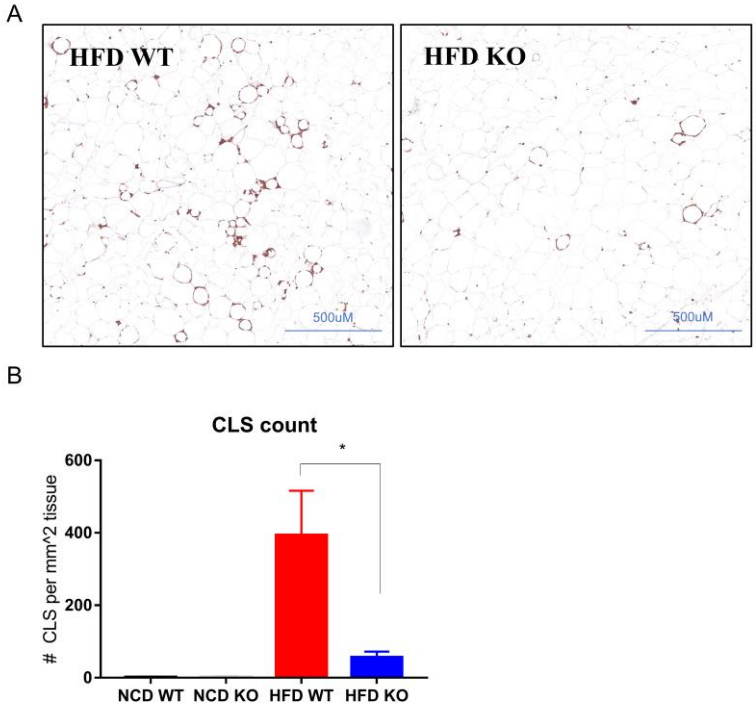

Figure 7. UCP2 deletion reduces eWAT macrophages after the HFD challenge.

(A) F4/80 IHC staining of crown-like structure (CLS) formation in eWAT.. (B) Number of CLS formation were graphed. Data are presented as the mean ± SEM. *$p < 0.05$, **$p < 0.01$, ***$p < 0.001$.

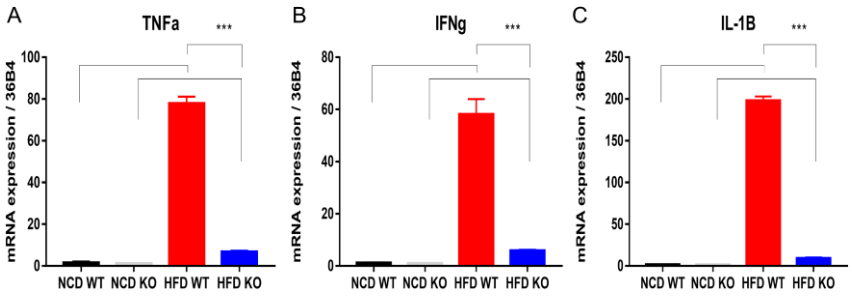

Figure 8. UCP2 deletion reduces pro-inflammatory marker expressions after the HFD challenge.

qRT-PCR analysis showed relative mRNA expression of pro-inflammatory markers, (A) TNFα, (B) IFN-γ, (C) IL-β. Data are presented as the mean ± SEM. *$p < 0.05$, **$p < 0.01$, ***$p < 0.001$.

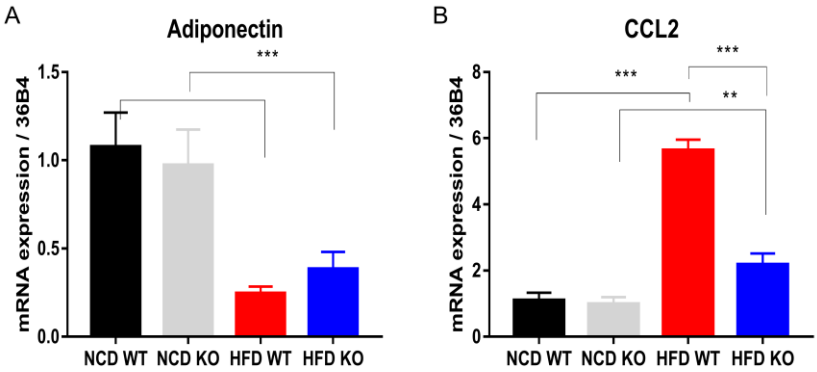

Figure 9. UCP2 deletion reduces anti-inflammatory marker expressions after the HFD challenge.

qRT-PCR analysis showed relative mRNA expressions of anti-inflammatory markers, (A) adiponectin, (B) IL-10. (C) Relative mRNA expression of macrophage infiltration marker CCL2. Data are presented as the mean ± SEM. *$p < 0.05$, **$p < 0.01$, ***$p < 0.001$.

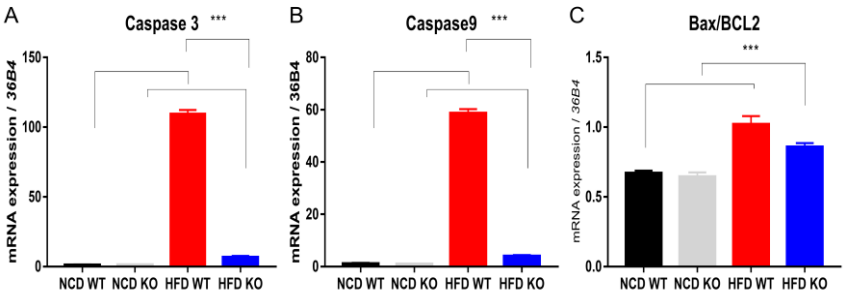

Figure 10. UCP2 deletion reduces apoptosis marker expressions in RNA level.

qRT-PCR analysis showed relative mRNA expression levels of apoptosis markers were analyzed in eWAT, (A) caspase 3, (B) Caspase 9, (C) Bax/BCL2. Data are presented as the mean ± SEM. *$p < 0.05$, **$p < 0.01$, ***$p < 0.001$.

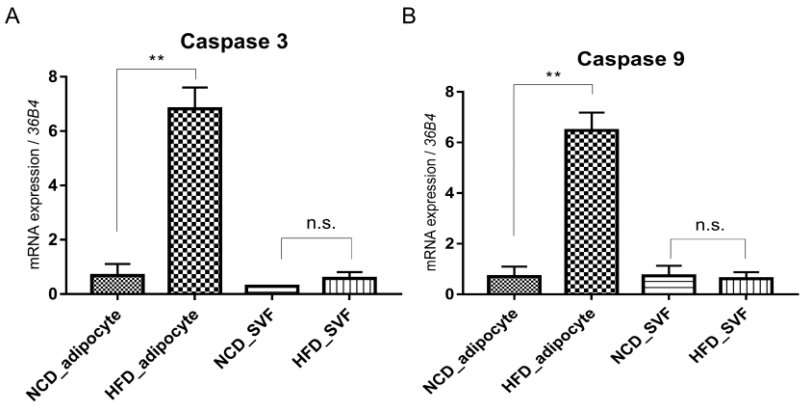

Figure 11. Apoptosis marker expression in adipocytes and SVF of HFD challenged B6 mice.

qRT-PCR analysis showed relative mRNA expression levels of apoptosis markers, (A) caspase 3, (B) caspase 9. Data are presented as the mean ± SEM. *$p < 0.05$, **$p < 0.01$, ***$p < 0.001$.

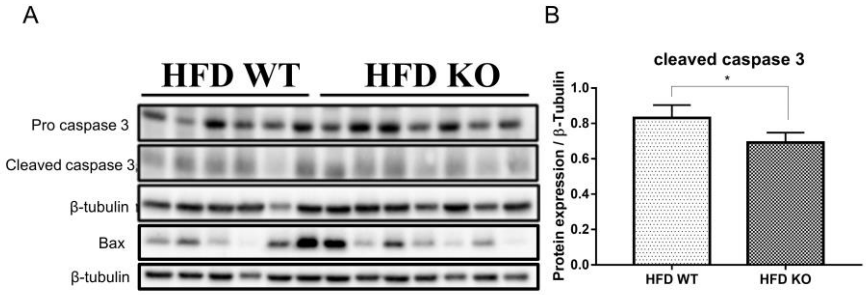

Figure 12. UCP2 deletion reduces apoptosis marker expressions in protein level.

(A) Protein expression of apoptosis marker in eWAT. (B) cleaved caspase 3 was quantified by ImageJ.

A

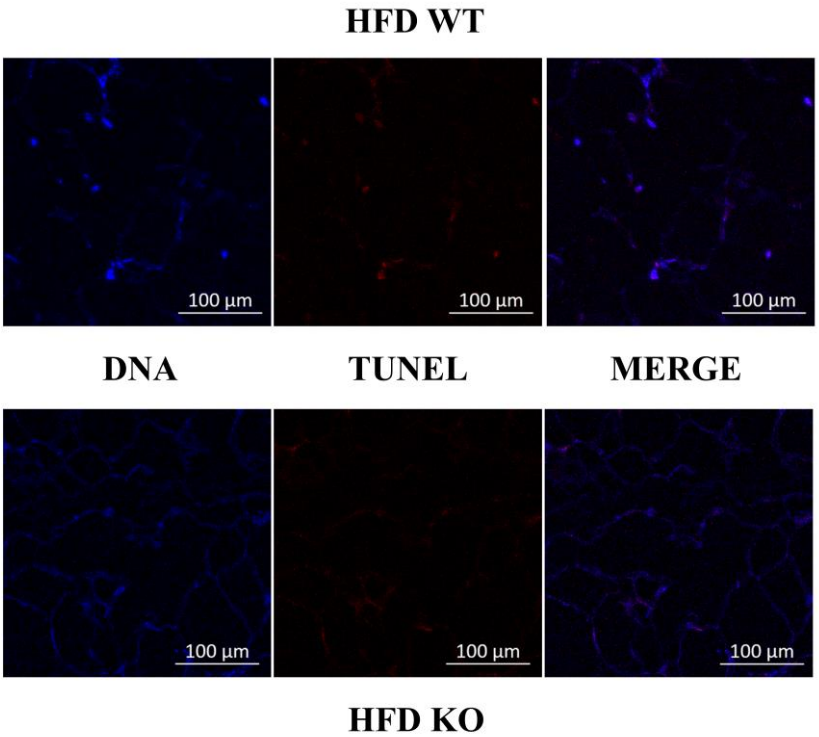

Figure 13. TUNEL assay shows reduced apoptosis in UCP2 KO mice.

(A) TUNEL assay in eWAT of HFD WT and KO mice.

Under β3 adrenergic receptor stimulation, UCP2 does not affect a thermogenic capacity

To stimulate the β3 adrenergic receptor, I injected CL 316,243, a β3 adrenergic agonist, intraperitoneally (i.p.) into 7-week-old mice, once a day (1 mg/kg) for three consecutive days. A schematic is shown in Fig. 14A. Body weight gains or losses were measured before the first injection and at the time of euthanasia. Saline-injected WT and KO mice gained comparable weights, whereas CL-injected KO mice lost significantly more weight than CL-injected WT mice did (Fig. 14B). The body compositions were also measured; fat content of CL-injected KO mice tended to be lower than that of CL-injected WT mice, but these differences were not statistically significant (Fig. 15A), while lean masses were similar among all groups (Fig. 15B). Their WAT masses were measured and normalized by their body weights and weights were recorded (Fig. 15C, 15D). I then measured browning of inguinal iWAT at the molecular level. Saline-injected WT and KO mice showed insignificant levels of UCP1, whereas CL-injected WT and KO mice both showed high expression of UCP1, at comparable levels (Fig. 16A, 16B). The mRNA levels of the browning markers, *UCP1*, *Elovl3*, *CIDEA*, and *PGC1α*, were consistent with the corresponding protein levels (Fig. 16C). Finally, I histologically investigated the browning of adipose

tissue and confirmed that adipocyte sizes, lipid droplet accumulations, and UCP1 expressions were similar between the two genotypes (Fig. 17,18).

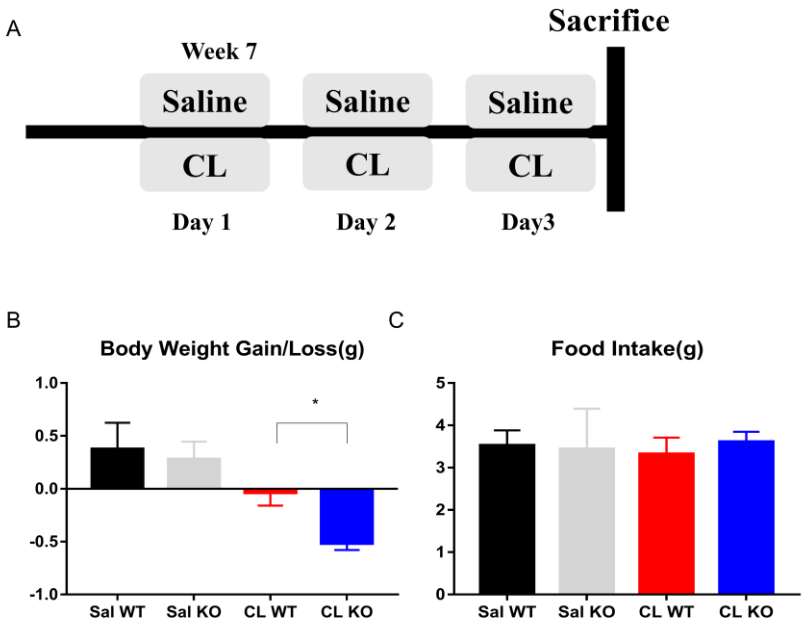

Figure 14. Inducing browning of WAT through β3 adrenergic stimulation by CL 316,243.

(A) Schematic diagram of CL injection experiment. (B) Net body weight gain and loss graph. (C) Amount of food consumption during the experiment. Data are presented as the mean ± SEM. *$p < 0.05$, **$p < 0.01$, ***$p < 0.001$.

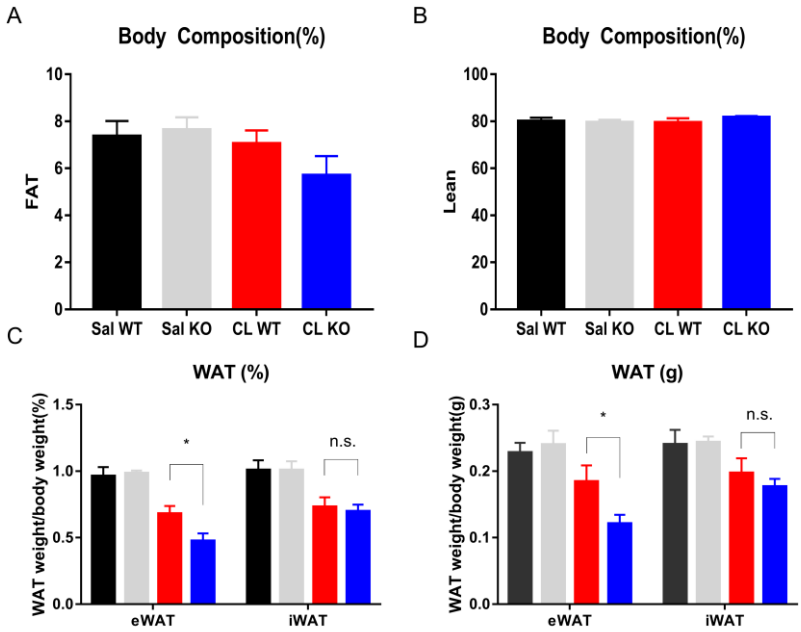

Figure 15. UCP2 deletion tends to reduce fat mass after CL injection.

Body composition data after CL injection, (A) FAT composition, (B) lean composition. (C) WAT weights normalized by total body weights. (D) WAT weights. Data are presented as the mean ± SEM. *$p < 0.05$, **$p < 0.01$, ***$p < 0.001$.

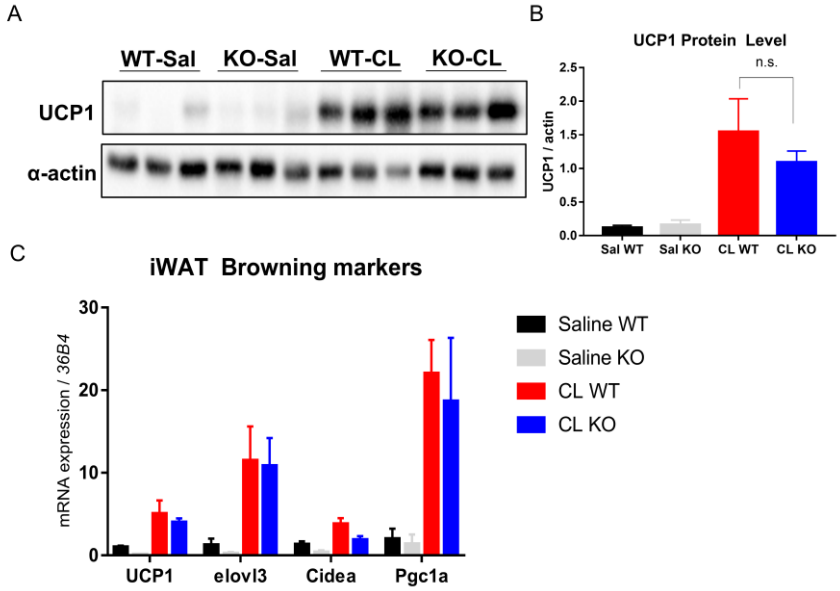

Figure 16. UCP2 deletion does not affect browning marker expressions after CL injection.

(A) UCP1 protein expression in iWAT and (B) the blot was quantified by ImageJ. (C) qRT-PCR showed relative mRNA expressions of browning markers. Data are presented as the mean ± SEM. *$p < 0.05$, **$p < 0.01$, ***$p < 0.001$.

A

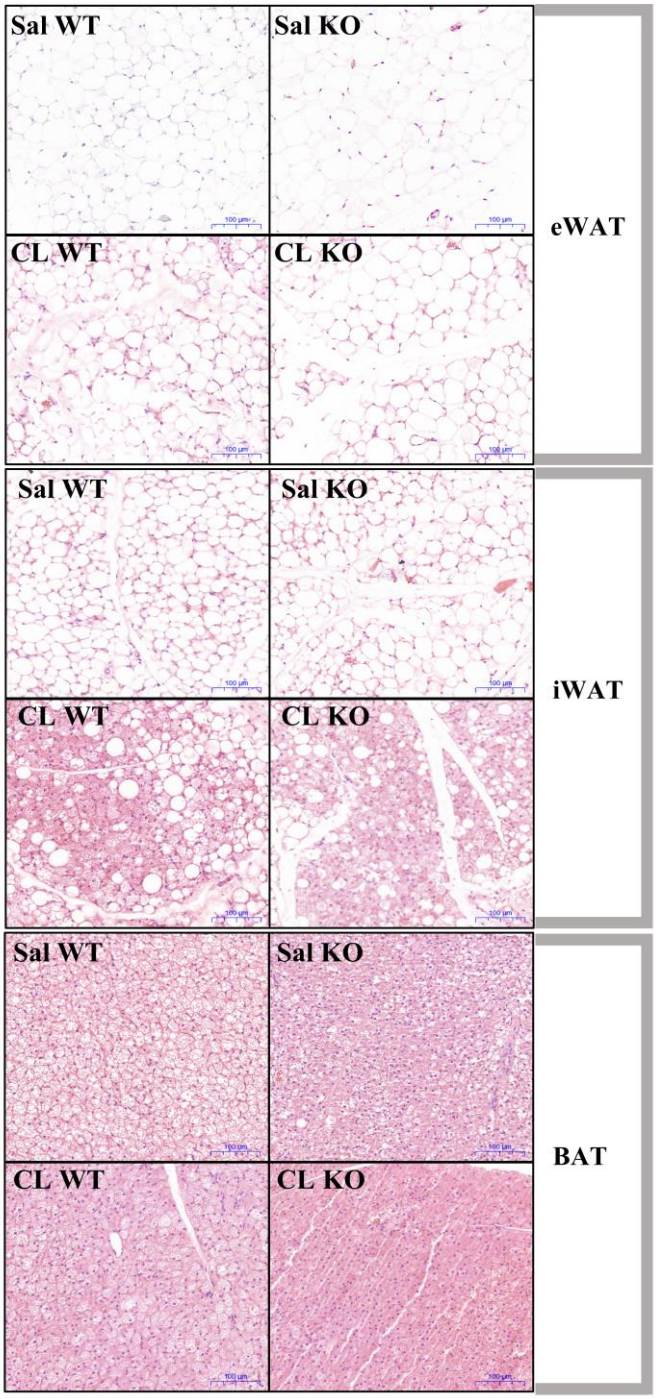
Sal WT
Sal KO
CL WT
CL KO
eWAT
Sal WT
Sal KO
CL WT
CL KO
iWAT
Sal WT
Sal KO
CL WT
CL KO
BAT

Figure 17. UCP2 deletion does not affect adipocyte sizes after CL injection.
(A) Relative mRNA expressions of browning markers were increased by the CL effect only.

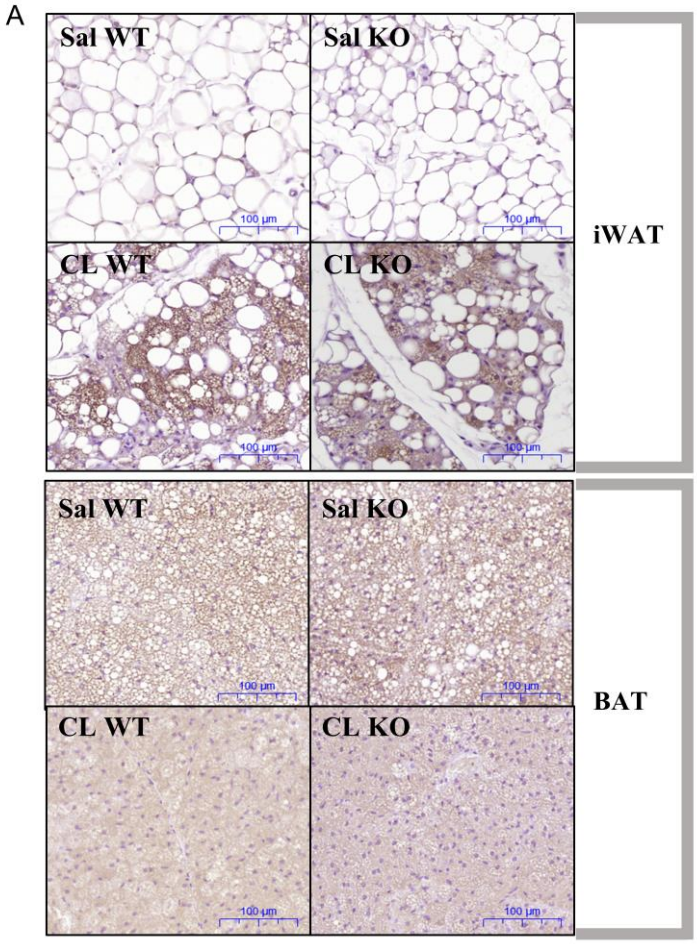

Figure 18 UCP2 deletion does not affect the browning of WAT and activation of BAT after the CL injection. (A) UCP1 expressions in iWAT and BAT were increased by the CL effect only.

UCP2 deletion does not affect phenotypes or browning of WAT under cold adaptation

To explore the role of UCP2 in cold adaptation, 7-week-old mice were expose to warm (30 °C) and cold (4 °C) conditions for 5 days. A schematic is shown in Fig. 18A. This cold exposure did not affect body weight changes in WT and KO mice (Fig. 18B). Changes in body composition data and WAT weight were negligible (Fig. 19A-19D). Protein and mRNA levels of browning markers showed similar cold effects in both the WT and KO groups and showed no differences between the two genotypes (Fig. 20A-20C). Finally, I compared histological differences, however; I found no evidence that UCP2 deletion affects adipose tissue remodeling (Fig. 21, 22).

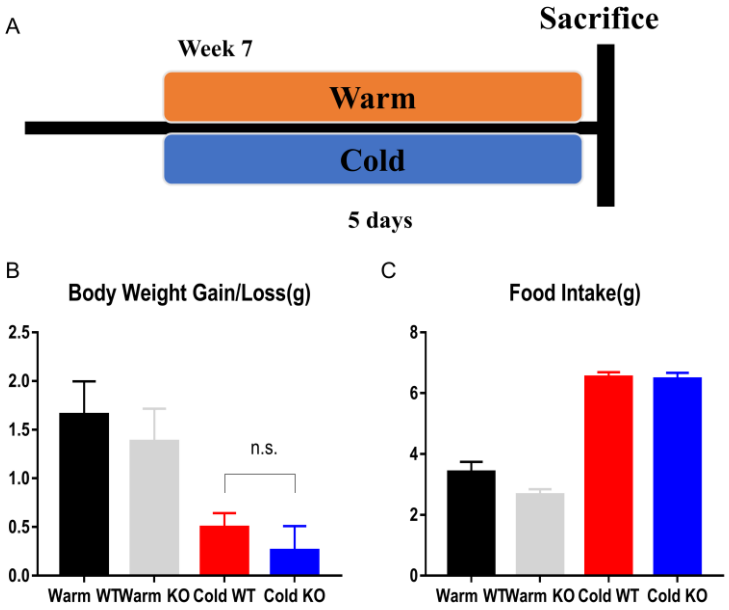

Figure 19. Inducing browning of WAT through β3 adrenergic stimulation by cold exposure.

(A) Schematic diagram of cold-induced browning. (B) Bodyweight changes induced by cold exposure were similar in both genotypes. (C) Food intake was similar. Data are presented as the mean ± SEM. *$p < 0.05$, **$p < 0.01$, ***$p < 0.001$.

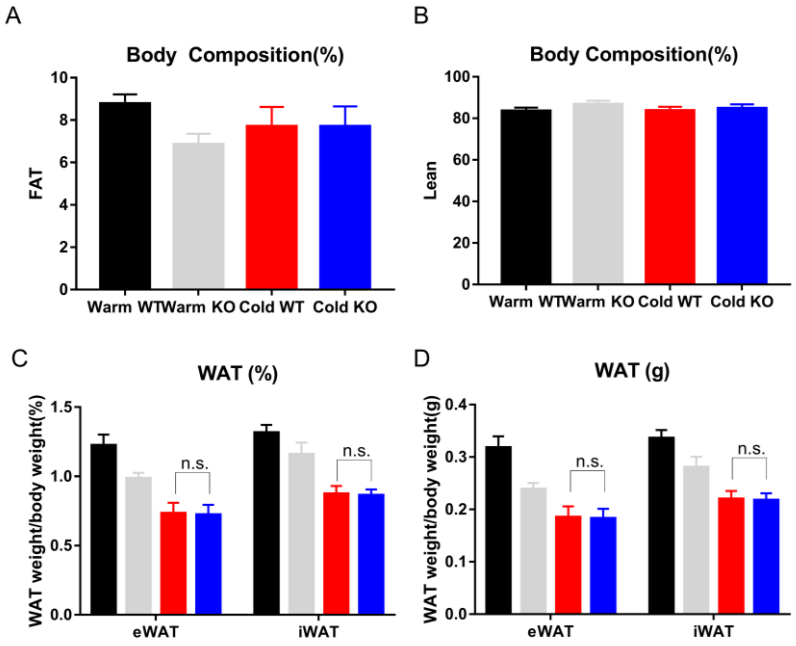

Figure 20. UCP2 deletion does not affect fat mass after cold exposure.

Body composition data after cold exposure, (A) FAT composition, (B) lean composition. (C) WAT weights normalized by total body weights. (D) WAT weights. Data are presented as the mean ± SEM. *$p < 0.05$, **$p < 0.01$, ***$p < 0.001$.

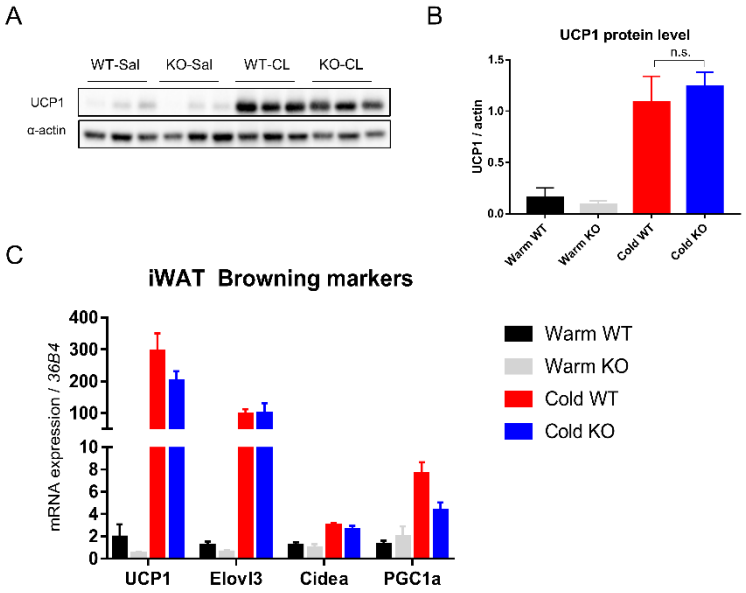

Figure 21. UCP2 deletion does not affect browning marker expressions after cold exposure.

(A) UCP1 protein expression in iWAT and (B) the blot was quantified by ImageJ. (C) qRT-PCR analysis showed relative mRNA expressions of browning markers. Data are presented as the mean ± SEM. *$p < 0.05$, **$p < 0.01$, ***$p < 0.001$.

A

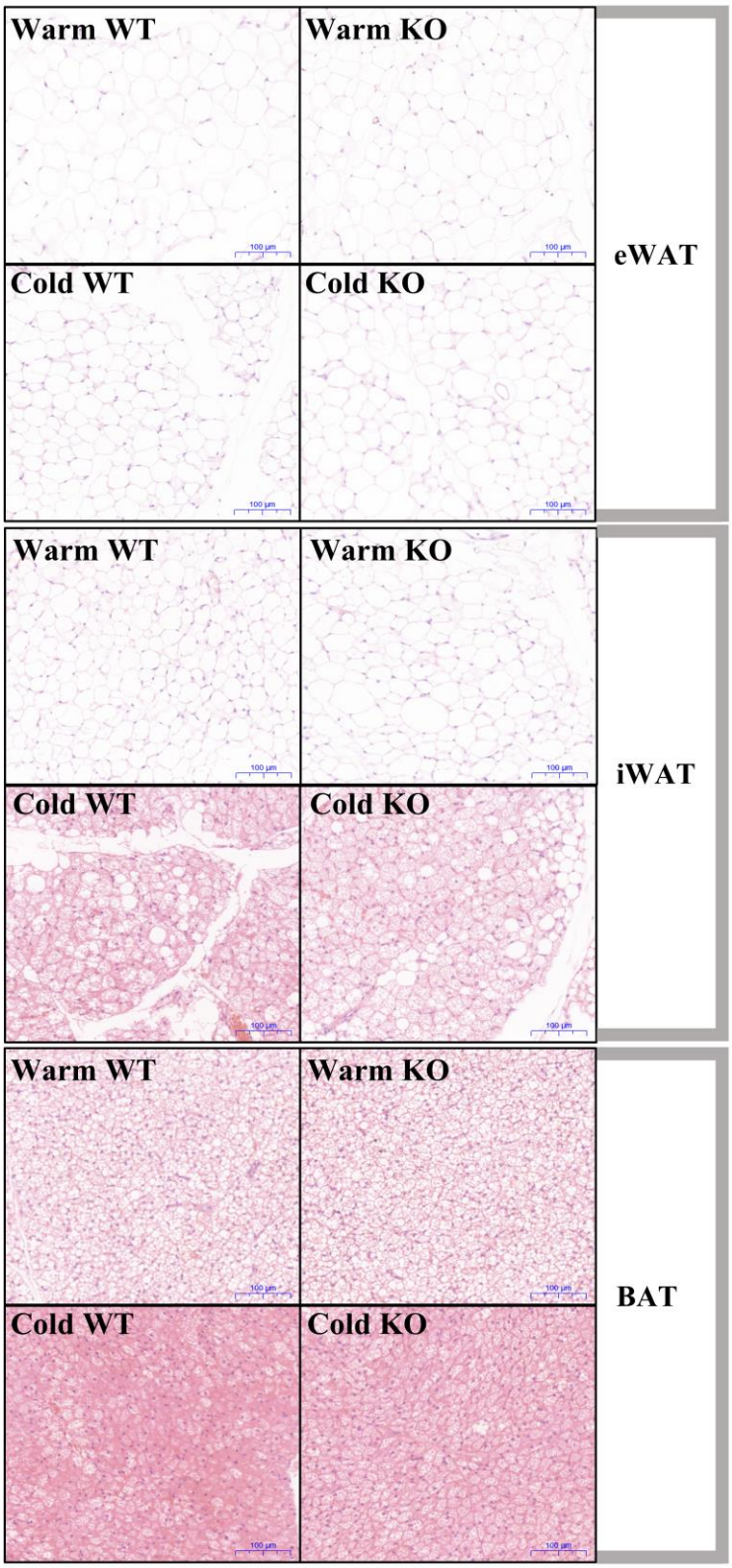
Warm WT
Warm KO
Cold WT
Cold KO
eWAT
Warm WT
Warm KO
Cold WT
Cold KO
iWAT
Warm WT
Warm KO
Cold WT
Cold KO
BAT

Figure 22. UCP2 deletion does not affect adipocyte sizes after cold exposure.

(A) H&E staining of eWAT, iWAT, and BAT.

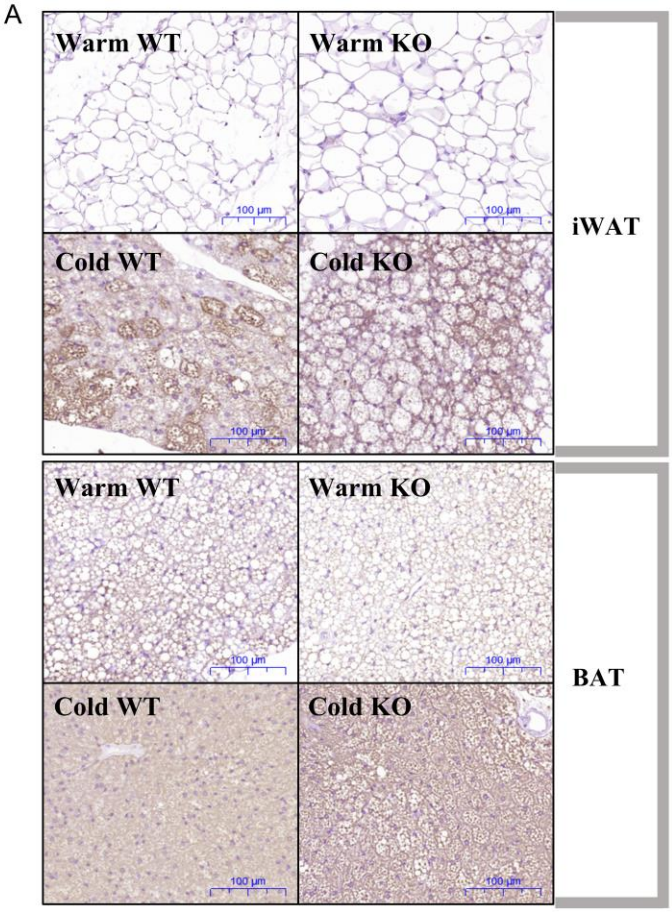

Figure 23. UCP2 deletion does not affect the browning of WAT and activation of BAT after the cold exposure. (A) UCP1 expressions in iWAT and BAT were increased by the cold effect only.

DISCUSSION

In the past decades, studies have revealed the significance of genes from *UCP* family. *UCP1* is specifically expressed in brown and beige adipocytes, *UCP3* expression is distributed in skeletal muscles, and *UCP2* expression has a wide tissue distribution (Erlanson-Albertsson, 2002). Many studies have studied the roles of UCP2 in various organs (Kim et al., 2015; Madreiter-Sokolowski et al., 2017; Qin et al., 2019) and//// studies demonstrated that UCP2 negatively regulates ROS formation (Andrews & Horvath, 2009; Arsenijevic et al., 2000; Bai et al., 2005). However, the role of UCP2 in adipose tissue and energy metabolism was not fully investigated.

In 2001, a cross between UCP2 KO and ob/ob mice was studied, which showed a gain of weight comparable to that of WT mice (Zhang et al., 2001). In 2002, UCP2 KO mice were reported to have higher body weights than WT mice after the HFD challenge (Joseph et al., 2002). These results contradict my observation that UCP2 KO mice gained significantly less weight than UCP2 WT mice did after the HFD challenge. These discrepancies may be attributed to two reasons. Firstly, the UCP2 KO mice used in each experiment had different backgrounds. In 2009, Pi *et al.* discovered that the insulin secretion capacities of UCP2

KO mice differed according to their genetic backgrounds (Pi et al., 2009). Among 129/B6 mixed, 129 congenic, B6 congenic, and A/J congenic UCP2 KO mice, only 129/B6 mixed genetic background, the one used in the two previously reported articles, showed a higher insulin secretion compared to WT mice. Lastly, all three articles used different experimental designs. Ob/ob mice with NCD were used for the first group, and 4-month-old mice were fed HFD for 4.5 months in the second group. 6-week-old mice fed HFD for 2 months were used for my experiment. I suggest that these two differences may have resulted in the inconsistent results of the studies.

Adipose tissue is a metabolically active and dynamic organ that comprises heterogeneous cell population (Eto et al., 2009). Adipocytes, making up the majority of cell populations, store energy in the form of triglycerides (Cohen & Spiegelman, 2016) whereas the rest of the populations are composed of various cell types, including immune cells (Bora & Majumdar, 2017; Eto et al., 2009; Prunet-Marcassus et al., 2006; Rondini & Granneman, 2020). Recently, a study has reported that macrophage-specific *UCP2* deletion does not affect body weight gain and adipose tissue inflammation after HFD (van Dierendonck et al., 2020), whereas my data demonstrated that *UCP2* null KO mice were

protected from DIO. To delineate this matter, I fed 6-week-old C57/BL6 mice HFD for short (2 weeks) and long (16 weeks) terms and isolated them into adipocytes and a SVF from eWAT. Although the *UCP2* mRNA levels in adipocytes and SVF of the NCD group were comparable, after the HFD challenge, adipocytes exhibited significantly higher *UCP2* levels than the SVF (Fig. 1A, Supplementary Fig. 1E). In addition, I used 3T3-L1 murine pre-adipocytes and confirmed that *UCP2* mRNA expression was increased by the *PGC1α* mRNA level, a marker for differentiation (Fig. 1B, C). Considering the expression levels of UCP2 in adipocytes, it may play a role in adipocytes but not in SVF, including macrophages, in HFD-induced obesity.

I induced obesity in UCP2 WT and KO mice through HFD. Surprisingly, HFD treated KO mice exhibited leaner phenotypes compared to WT mice. Weight gain was significantly reduced in UCP2 KO mice compared to that in WT mice (Fig. 1D-F). Serum TG and glucose levels were significantly lower in the HFD KO group (Supplementary Fig. 1G, H), and the eWAT glucose uptake marker level was also reduced in HFD KO mice (Supplementary Fig. 1L). HFD KO mice had significantly lower fat content (Fig. 1G) and WAT weights (Fig. 1I). Histologically, HFD KO mice showed smaller adipocyte distribution (Fig. 1J, K).

Obesity is strongly associated with pro-inflammatory cytokines and adipose tissue macrophages (Wang et al., 2021; Weisberg et al., 2003). Moreover, deletion of macrophages has been reported to prevent DIO phenotypes in eWAT (Bu et al., 2013). It has also been reported that adipocyte apoptosis is an upstream event necessary for macrophage infiltration into adipose tissue and CLS formation (Alkhouri et al., 2010; Lindhorst et al., 2021; Xiao et al., 2010). Furthermore, UCP2 was reported to regulate adipocyte apoptosis in 3T3L1 cell lines when treated with 1alpha,25-dihydroxyvitamin D3 (Sun & Zemel, 2004). I confirmed that adipose tissue macrophages (Fig. 2A, B) and pro-inflammatory markers (Fig. 2C) were reduced in HFD KO mice than in HFD WT mice. I then compared apoptosis between the two genotypes. Interestingly, HFD KO mice showed significantly reduced mRNA and protein expression of apoptosis markers compared to HFD WT mice (Fig. 2F, Supplementary Fig. 1H, I). TUNEL assay also showed higher apoptotic signals in the HFD WT group (Supplementary Fig. 1K).

Sympathetic nervous system stimulation via β-adrenergic receptors induces multilocular lipid droplets in adipocytes and browning of white adipose tissue. UCP1, a well-known marker for browning of WAT, dissipates heat by uncoupling the H+ gradient, which would otherwise

be used in ATP synthesis. Recently, Caron S *et al.* reported that UCP2 KO mice failed to adapt to chronic cold exposure (10 °C) (Caron et al., 2017). This study focused on glucose metabolism in BAT and did not reveal the role of UCP2 in iWAT and thermogenesis. Here, using stimulation with a β3 adrenergic agonist and 4 °C cold exposure, I demonstrated that the browning capacity of iWAT is comparable between WT and KO mice. UCP2-depleted mice showed a tendency to lose more weight than WT mice (Fig. 3B, 4B), but the weights of WAT and adipocyte sizes were comparable (Fig. 3F, I; 4F, I). Moreover, the protein and mRNA expression of major browning markers in iWAT were comparably increased (Fig. 3G, H; 4G, H).

In conclusion, UCP2 deficiency ameliorated HFD-induced obesity in eWAT but did not alter thermogenic and browning capacities in iWAT. HFD-challenged UCP2 KO mice showed lean phenotypes in terms of body weight, fat composition, fat weights, and smaller adipocytes, Additionally, macrophage infiltration, CLS formation, pro-inflammatory cytokine markers, and apoptosis markers were reduced in the eWAT of the HFD KO mice. Considering the high expression levels of UCP2 in HFD adipocytes, I suggest that UCP2 may regulate apoptotic pathways of adipocytes and eventually prevent HFD-induced obesity.

CONCLUSIONS

UCP2 expression increases as 3T3L1 cell line differentiates, so I tried to explore the role of UCP2 in murine adipose tissue. HFD challenge increases UCP2 expression in adipocytes rather than in SVF. Also, UCP2 KO mice maintained lean body and fat weights after HFD challenge compared to WT mice. Number of adipose tissue-infiltrated macrophages and inflammation marker expression were downregulated in KO mice. More importantly, adipocyte apoptosis was reduced in KO mice which induces macrophage infiltration. In this paper, I suggest that UCP2 KO mice were protected from diet-induced obesity by inhibition of adipocyte apoptosis.

REFERENCES

Alkhouri, N., Gornicka, A., Berk, M. P., Thapaliya, S., Dixon, L. J., Kashyap, S., Schauer, P. R., & Feldstein, A. E. (2010). Adipocyte apoptosis, a link between obesity, insulin resistance, and hepatic steatosis. *J Biol Chem*, *285*(5), 3428-3438.

Andrews, Z. B., & Horvath, T. L. (2009). Uncoupling protein-2 regulates lifespan in mice. *Am J Physiol Endocrinol Metab*, *296*(4), E621-627.

Arsenijevic, D., Onuma, H., Pecqueur, C., Raimbault, S., Manning, B. S., Miroux, B., Couplan, E., Alves-Guerra, M. C., Goubern, M., Surwit, R., Bouillaud, F., Richard, D., Collins, S., & Ricquier, D. (2000). Disruption of the uncoupling protein-2 gene in mice reveals a role in immunity and reactive oxygen species production. *Nat Genet*, *26*(4), 435-439.

Bai, Y., Onuma, H., Bai, X., Medvedev, A. V., Misukonis, M., Weinberg, J. B., Cao, W., Robidoux, J., Floering, L. M., Daniel, K. W., & Collins, S. (2005). Persistent nuclear factor-kappa B activation in UCP2-/- mice leads to enhanced nitric oxide and inflammatory cytokine production. *J Biol Chem*, *280*(19), 19062-19069.

Bartelt, A., & Heeren, J. (2014). Adipose tissue browning and metabolic health. *Nat Rev Endocrinol*, *10*(1), 24-36.

Bora, P., & Majumdar, A. S. (2017). Adipose tissue-derived stromal vascular fraction in regenerative medicine: a brief review on

biology and translation. *Stem Cell Res Ther*, *8*(1), 145.

Bu, L., Gao, M., Qu, S., & Liu, D. (2013). Intraperitoneal injection of clodronate liposomes eliminates visceral adipose macrophages and blocks high-fat diet-induced weight gain and development of insulin resistance. *AAPS J*, *15*(4), 1001-1011.

Caron, A., Labbe, S. M., Carter, S., Roy, M. C., Lecomte, R., Ricquier, D., Picard, F., & Richard, D. (2017). Loss of UCP2 impairs cold-induced non-shivering thermogenesis by promoting a shift toward glucose utilization in brown adipose tissue. *Biochimie*, *134*, 118-126.

Choe, S. S., Huh, J. Y., Hwang, I. J., Kim, J. I., & Kim, J. B. (2016). Adipose Tissue Remodeling: Its Role in Energy Metabolism and Metabolic Disorders. *Front Endocrinol (Lausanne)*, *7*, 30.

Cohen, P., & Spiegelman, B. M. (2016). Cell biology of fat storage. *Mol Biol Cell*, *27*(16), 2523-2527.

Erlanson-Albertsson, C. (2002). Uncoupling proteins--a new family of proteins with unknown function. *Nutr Neurosci*, *5*(1), 1-11.

Eto, H., Suga, H., Matsumoto, D., Inoue, K., Aoi, N., Kato, H., Araki, J., & Yoshimura, K. (2009). Characterization of structure and cellular components of aspirated and excised adipose tissue. *Plast Reconstr Surg*, *124*(4), 1087-1097.

Fedorenko, A., Lishko, P. V., & Kirichok, Y. (2012). Mechanism of fatty-

acid-dependent UCP1 uncoupling in brown fat mitochondria. *Cell*, *151*(2), 400-413.

Himms-Hagen, J. (1985). Brown adipose tissue metabolism and thermogenesis. *Annu Rev Nutr*, *5*, 69-94.

Joseph, J. W., Koshkin, V., Zhang, C. Y., Wang, J., Lowell, B. B., Chan, C. B., & Wheeler, M. B. (2002). Uncoupling protein 2 knockout mice have enhanced insulin secretory capacity after a high-fat diet. *Diabetes*, *51*(11), 3211-3219.

Kim, J. G., Sun, B. H., Dietrich, M. O., Koch, M., Yao, G. Q., Diano, S., Insogna, K., & Horvath, T. L. (2015). AgRP Neurons Regulate Bone Mass. *Cell Rep*, *13*(1), 8-14.

Lee, M. J., Wu, Y., & Fried, S. K. (2013). Adipose tissue heterogeneity: implication of depot differences in adipose tissue for obesity complications. *Mol Aspects Med*, *34*(1), 1-11.

Lindhorst, A., Raulien, N., Wieghofer, P., Eilers, J., Rossi, F. M. V., Bechmann, I., & Gericke, M. (2021). Adipocyte death triggers a pro-inflammatory response and induces metabolic activation of resident macrophages. *Cell Death Dis*, *12*(6), 579.

Madreiter-Sokolowski, C. T., Gyorffy, B., Klec, C., Sokolowski, A. A., Rost, R., Waldeck-Weiermair, M., Malli, R., & Graier, W. F. (2017). UCP2 and PRMT1 are key prognostic markers for lung carcinoma patients. *Oncotarget*, *8*(46), 80278-80285.

Madsen, L., Pedersen, L. M., Lillefosse, H. H., Fjaere, E., Bronstad, I., Hao, Q., Petersen, R. K., Hallenborg, P., Ma, T., De Matteis, R., Araujo, P., Mercader, J., Bonet, M. L., Hansen, J. B., Cannon, B., Nedergaard, J., Wang, J., Cinti, S., Voshol, P., . . . Kristiansen, K. (2010). UCP1 induction during recruitment of brown adipocytes in white adipose tissue is dependent on cyclooxygenase activity. *PLoS One*, *5*(6), e11391.

Pi, J., Bai, Y., Daniel, K. W., Liu, D., Lyght, O., Edelstein, D., Brownlee, M., Corkey, B. E., & Collins, S. (2009). Persistent oxidative stress due to absence of uncoupling protein 2 associated with impaired pancreatic beta-cell function. *Endocrinology*, *150*(7), 3040-3048.

Prunet-Marcassus, B., Cousin, B., Caton, D., Andre, M., Penicaud, L., & Casteilla, L. (2006). From heterogeneity to plasticity in adipose tissues: site-specific differences. *Exp Cell Res*, *312*(6), 727-736.

Qin, N., Cai, T., Ke, Q., Yuan, Q., Luo, J., Mao, X., Jiang, L., Cao, H., Wen, P., Zen, K., Zhou, Y., & Yang, J. (2019). UCP2-dependent improvement of mitochondrial dynamics protects against acute kidney injury. *J Pathol*, *247*(3), 392-405.

Rondini, E. A., & Granneman, J. G. (2020). Single cell approaches to address adipose tissue stromal cell heterogeneity. *Biochem J*, *477*(3), 583-600.

Sun, X., & Zemel, M. B. (2004). Role of uncoupling protein 2 (UCP2) expression and 1alpha, 25-dihydroxyvitamin D3 in modulating adipocyte apoptosis. *FASEB J*, *18*(12), 1430-1432.

Trayhurn, P. (2007). Adipocyte biology. *Obes Rev*, *8 Suppl 1*, 41-44.

van Dierendonck, X., Sancerni, T., Alves-Guerra, M. C., & Stienstra, R. (2020). The role of uncoupling protein 2 in macrophages and its impact on obesity-induced adipose tissue inflammation and insulin resistance. *J Biol Chem*, *295*(51), 17535-17548.

Wang, Y., Tang, B., Long, L., Luo, P., Xiang, W., Li, X., Wang, H., Jiang, Q., Tan, X., Luo, S., Li, H., Wang, Z., Chen, Z., Leng, Y., Jiang, Z., Wang, Y., Ma, L., Wang, R., Zeng, C., . . . Shi, C. (2021). Improvement of obesity-associated disorders by a small-molecule drug targeting mitochondria of adipose tissue macrophages. *Nat Commun*, *12*(1), 102.

Weisberg, S. P., McCann, D., Desai, M., Rosenbaum, M., Leibel, R. L., & Ferrante, A. W., Jr. (2003). Obesity is associated with macrophage accumulation in adipose tissue. *J Clin Invest*, *112*(12), 1796-1808.

Xiao, Y., Yuan, T., Yao, W., & Liao, K. (2010). 3T3-L1 adipocyte apoptosis induced by thiazolidinediones is peroxisome proliferator-activated receptor-gamma-dependent and mediated by the caspase-3-dependent apoptotic pathway. *FEBS J*, *277*(3), 687-696.

Zhang, C. Y., Baffy, G., Perret, P., Krauss, S., Peroni, O., Grujic, D., Hagen, T., Vidal-Puig, A. J., Boss, O., Kim, Y. B., Zheng, X. X., Wheeler, M. B., Shulman, G. I., Chan, C. B., & Lowell, B. B. (2001).

Uncoupling protein-2 negatively regulates insulin secretion and is a major link between obesity, beta cell dysfunction, and type 2 diabetes. *Cell*, *105*(6), 745-755.

국문 초록

UCP2 결손 마우스의 지방세포 사멸 억제 및 항 비만 연구

서울대학교 대학원
수의학과 수의생명과학전공
(발생유전학)

김 도 현

(지도교수: 성 제 경)

국문초록

Uncoupling Protein 2(UCP2)는 **Uncoupling Protein Family**의 구성원이자 **ROS** 형성의 조절자로 처음 알려졌지만 지방 조직에서의 역할은 아직 정확하게 알려지지 않았습니다. 이번 연구를 통해 고지방식이를 통해 비만이나 백색 지방의 갈색화를 유도할 때 **UCP2**의 역할을 보았습니다. 고지방식이로 비만이 유도되는 과정에서 백색지방으로 대식세포들이 침투하여 지방세포를 둘러싸고 왕관과 같은 구조**(CLS)**를 형성하며 포식을 하고 그 과정 중에 전 염증성 사이토카인을 다량 분비한다고 잘 알려져 있습니다. 일부 보고서에 따르면 큰 포식세포**(macrophage)**들은 사멸하는 지방세포들을 둘러싸며 **CLS**를 형성하게 됩니다. 이 과정 중에 **UCP2**의 역할을 알고자, 정상 마우스와 **UCP2** 결손 마우스에 고지방식이를 통해 비만을 유도하였습니다. 그 결과, 결손 마우스가 정상 마우스에 비해 상대적으로 살이 덜 찌는 표현형을 보였습니다. **HFD WT** 마우스에 비해 **HFD KO** 마우스에서 큰 포식세포 침투, **CLS** 형성 및 전 염증성 사이토카인이 감소했습니다. 또한 놀랍게도, **UCP2 KO** 마우스에서도 세포자살 신호가 감소되어 있는 것을 확인하였습니다. 이번 연구에서는 **UCP2** 결핍이 지방 세포 사멸을 조절하여 고지방식이에 의한 비만을 예방할 수 있음을 시사합니다. 그러나 **UCP2**가 결손 되더라도 정상 마우스와 비슷한 백색지

방의 갈색화 능력을 보여 주었습니다.

주요 단어: **Uncoupling Protein 2**, 비만, 지방 조직 염증, **CLS**, 마우스, 세포 사멸

학번: **2020-23775**